THE JOURNAL OF BIOLOGICAL CHEMISTRY VOL. 285, NO. 7, pp. 4975–4982, February 12, 2010

Transforming Growth Factor-β Regulates Basal Transcriptional Regulatory Machinery to Control Cell Proliferation and Differentiation in Cranial Neural Crest-derived Osteoprogenitor Cells*[S]

Received for publication, June 19, 2009, and in revised form, December 1, 2009 Published, JBC Papers in Press, December 3, 2009, DOI 10.1074/jbc.M109.035105

Jun-ichi Iwata[‡], Ryoichi Hosokawa[‡], Pedro A. Sanchez-Lara[§], Mark Urata[‡§], Harold Slavkin[‡], and Yang Chai[‡1]

From the [‡]Center for Craniofacial Molecular Biology, School of Dentistry, University of Southern California, Los Angeles, California 90033 and the [§]Division of Plastic Surgery, Childrens Hospital Los Angeles, Los Angeles, California 90027

Transforming growth factor-β (Tgf-β) signaling is crucial for regulating craniofacial development. Loss of Tgf-β signaling results in defects in cranial neural crest cells (CNCC), but the mechanism by which Tgf-β signaling regulates bone formation in CNCC-derived osteogenic cells remains largely unknown. In this study, we discovered that Tgf-β regulates the basal transcriptional regulatory machinery to control intramembranous bone development. Specifically, basal transcription factor *Taf4b* is down-regulated in the CNCC-derived intramembranous bone in *Tgfbr2*$^{fl/fl}$;*Wnt1-Cre* mice. Tgf-β specifically induces *Taf4b* expression. Moreover, small interfering RNA knockdown of *Taf4b* results in decreased cell proliferation and altered osteogenic differentiation in primary mouse embryonic maxillary mesenchymal cells, as seen in *Tgfbr2* mutant cells. In addition, we show that Taf1 is decreased at the osteogenic initiation stage in the maxilla of *Tgfbr2* mutant mice. Furthermore, small interfering RNA knockdown of *Taf4b* and *Taf1* together in primary mouse embryonic maxillary mesenchymal cells results in up-regulated osteogenic initiator *Runx2* expression, with decreased cell proliferation and altered osteogenic differentiation. Our results indicate a critical function of Tgf-β-mediated basal transcriptional factors in regulating osteogenic cell proliferation and differentiation in CNCC-derived osteoprogenitor cells during intramembranous bone formation.

Craniofacial skeletal elements are mainly formed by intramembranous ossification through a mechanism that remains relatively uncharacterized. The majority of osteoblasts and chondrocytes in the craniofacial region are derived from cranial neural crest cells (CNCC),[2] which produce the facial skeleton (1, 2). Tgf-β signaling plays a crucial role in craniofacial development, and loss of Tgf-β signaling in CNCC results in craniofacial skeletal malformations (3, 4).

Tgf-β transmits signals through a membrane receptor serine/threonine kinase complex that phosphorylates Smad2 and Smad3, and activated Smads form transcriptional complexes with Smad4 and translocate into the nucleus (5). These Tgf-β signaling complexes contain other transcription factors and target a variety of genes in an embryonic stage-dependent and cell type-specific manner, but the factors involved in this transcriptional regulatory machinery have yet to be identified. During development, the expression of many genes is associated with changes accompanied by dynamic restructuring of chromatin (6, 7). Recent studies demonstrate that basal transcriptional factors have cell- and promoter-specific functions during embryogenesis (8–12).

RNA polymerase II requires the assembly of a multiprotein complex around the transcriptional start site (13). The general transcriptional factor IID (TFIID) is a large multiprotein transcriptional factor, consisting of the TATA-binding protein and a set of 13–14 TATA-binding protein-associated factors (TAFs), that is responsible for specific binding to the TATA element found in many polymerase II promoters and also demonstrates a coactivator function during transcriptional initiation (14). TAFs are able to regulate gene transcription at multiple steps, with functions in promoter recognition, selective binding to core promoter elements, as well as direct interactions with transcriptional activators (15–17). Mutation and loss of TAFs in yeast and mammalian cells lead to cell cycle arrest and gene-specific transcriptional effects (16). The function of TAFs in gene regulation during embryogenesis has yet to be determined. Here, we show that the interaction between Tgf-β signaling and TAFs has a crucial role in regulating CNCC-derived osteogenesis during craniofacial morphogenesis.

EXPERIMENTAL PROCEDURES

Animals—Mating *Tgfbr2*$^{fl/+}$;*Wnt1-Cre* with *Tgfbr2*$^{fl/fl}$ mice generated *Tgfbr2*$^{fl/fl}$;*Wnt1-Cre* conditional null alleles that were genotyped using PCR primers as described previously (4).

Whole-mount Skeletal Staining—The three-dimensional architecture of the skeleton was examined using a modified whole-mount Alcian blue-Alizarin Red S staining protocol as described previously (3).

* This work was supported, in whole or in part, by National Institutes of Health Grants DE012711, DE014078, and U01 DE020065 from NIDCR (to Y. C.).

[S] The on-line version of this article (available at http://www.jbc.org) contains supplemental Figs. S1–S4.

[1] To whom correspondence should be addressed: Center for Craniofacial Molecular Biology, School of Dentistry, University of Southern California, 2250 Alcazar St., CSA 103, Los Angeles, CA 90033. Tel.: 323-442-3480; Fax: 323-442-2981; E-mail: ychai@usc.edu.

[2] The abbreviations used are: CNCC, cranial neural crest cells; JNK, Jun oncogene N-terminal kinase; MEMM, mouse embryonic maxillary mesenchymal; TAF, TATA-binding protein-associated factors; Tgf-β, transforming growth factor-β; siRNA, small interfering RNA; GAPDH, glyceraldehyde-3-phosphate dehydrogenase; RT, reverse transcription; TFIID, transcription factor IID; E, embryonic day.

Histological Examination—Hematoxylin and eosin staining and bromodeoxyuridine staining were performed as described previously (4, 18–20). Immunohistochemical staining was performed as described previously (18). Antibody used for immunohistochemistry was anti-Taf1 rabbit polyclonal antibodies (Abcam).

Immunological Analysis—Western blots were performed as described previously (21–23). Antibodies used for Western blotting were as follows: rabbit polyclonal antibodies against cyclin D1, cyclin D2, cyclin D3, cyclin A, cyclin E, JNK, and phospho-JNK (Cell Signaling Technology); FoxO4, FoxO3a, and Taf1 (Abcam); osteopontin, osteocalcin, and osteonectin (Santa Cruz Biotechnology); and mouse monoclonal antibody against GAPDH (Chemicon).

RNA Preparation and Quantitative RT-PCR—Total RNA was isolated from mouse embryonic maxilla dissected at the indicated developmental stage or from primary MEMM cells as described previously (24). First-strand cDNA was synthesized from 1 μg of total RNA using an oligo$(dT)_{20}$ primer and SuperScript III reverse transcriptase (Invitrogen), and quantitative PCR was performed in triplicate by SYBR Green (Bio-Rad) in an iCycler (Bio-Rad). A melting curve was obtained for each PCR product after each run to confirm that the SYBR Green signal corresponded to a unique and specific amplicon. The relative abundance of each transcript was calculated based on PCR efficiency and cycle number at which the fluorescence crosses a threshold for the GAPDH internal reference and the gene tested using iCycler iQ optical system software (Bio-Rad). PCR primers are available upon request.

In Situ Hybridization—To generate the probe for *in situ* hybridization of mouse *Taf4b*, DNA encoding *Taf4b* was amplified from E13.5 mouse maxilla cDNA by PCR. The PCR fragments were cloned into the pDrive cloning vector (Qiagen). All recombinant plasmids were verified by sequencing. *In situ* hybridization was performed as described previously (18). Several negative controls (*e.g.* sense probe and no probe) were run in parallel with the experimental reaction. Details of the experimental procedures are available upon request.

Organ Culture of Maxilla and Tgf-β Bead Implantation—Affi-Gel blue beads (Bio-Rad) were used for delivery of Tgf-β2. The beads were washed in phosphate-buffered saline and then incubated for 1 h at room temperature in 10 μg/ml Tgf-β2 (R & D Systems). Control beads were incubated with 0.1% bovine serum albumin. Tgf-β2- or bovine serum albumin-containing beads were placed adjacent to the maxilla.

Primary Cultured Cells Derived from Mouse Embryonic Maxillary Mesenchyme—Primary MEMM cells were obtained from 13.5-day-old embryos (E13.5). Briefly, maxilla was dissected at E13.5 and trypsinized for 30 min at 37 °C in a CO_2 incubator. After pipetting thoroughly, cells were cultured in Dulbecco's modified Eagle's medium containing 10% fetal bovine serum supplemented with penicillin, streptomycin, L-glutamate, sodium pyruvate, and nonessential amino acids. Proliferation of primary MEMM cells was measured using a cell counting kit 8 (Dojindo Molecular Technologies, Gaithersburg, MD). Primary MEMM cells (5×10^3 cells per well) were seeded into 96-well plates and incubated at 37 °C in a CO_2 incubator for up to 72 h. Following this incubation period, sodium 2-(4-iodophenyl)-3-(4-nitrophenyl)-5-(2,4-disulfophenyl)-2*H*-tetrazolium was added to the culture medium to label the proliferating cells, and incubation was continued for an additional 1 h at 37 °C. The amount of reduced tetrazolium was determined by measuring the absorbance at 450 nm in a microplate reader. Osteogenic differentiation was promoted by culture in monolayers after initial seeding of cells at 1.5×10^4 cells/cm^2 in complete medium supplemented with 10 mM β-glycerophosphate, 0.1 μM dexamethasone, and 0.05 mM ascorbic acid (Sigma) for 2 weeks. Alkaline phosphatase activity was measured as described previously (25).

Small Interfering RNA Transfection (siRNA)—MEMM cells (2×10^6 cells) were plated in a 6-well cell culture plate until the cells reached 60–80% confluence. siRNA duplex and reagents were purchased from Invitrogen and Santa Cruz Biotechnology, respectively. siRNA mixture in transfection medium was incubated with cells for 6 h at 37 °C in a CO_2 incubator, and then 5×10^3 cells were cultured for 2 weeks in regular or osteogenic differentiation medium, including siRNA transfection mixture. Specifically, siRNA was added every 3 days into the cell culture medium throughout the 2 weeks of culture.

Statistical Analysis—Two-tailed Student's *t* test was applied for statistical analysis. For all graphs, data are represented as mean ± S.D. A *p* value of less than 0.05 was considered statistically significant.

RESULTS

Loss of Tgfbr2 in Cranial Neural Crest Cells Results in Decreased Maxilla Size in Vivo—CNCC-derived osteogenic cells contribute to craniofacial bone formation that is developed through intramembranous bone ossification (1, 2). However, most facial skeletal bones are not ideal models for the analysis of intramembranous ossification. For instance, mandibular bone includes regions of both endochondral and intramembranous ossifications, and analysis of the skull region is complicated by its proximity to the dura mater. In this study, we analyzed the role of Tgf-β receptor type II in the maxilla to investigate intramembranous ossification derived from CNCC in the absence of other ossification processes or inductive tissues. The maxillary region is composed of six primordia as follows: pairs of premaxilla, maxilla, and palatine bones, which are all derived from CNCC. The size of the maxilla and palatine bones in newborn *Tgfbr2*$^{fl/fl}$;*Wnt1-Cre* mice was smaller than those of *Tgfbr2*$^{fl/fl}$ control mice (Fig. 1, *A–R*, *W*, and *X*). Palatal and frontal processes of maxillary bone were defective in *Tgfbr2*$^{fl/fl}$;*Wnt1-Cre* mice at E14.5 (Fig. 1, *S–V*). Thus, loss of Tgf-β signaling appears to affect intramembranous ossification.

Decreased Cell Proliferation and Altered Osteogenic Differentiation in the Maxilla of Tgfbr2$^{fl/fl}$*;Wnt1-Cre Mice*—To investigate the cellular mechanism of decreased maxilla size in *Tgfbr2*$^{fl/fl}$;*Wnt1-Cre* mice, we analyzed the rate of cellular proliferation and apoptosis relative to littermate wild type maxilla. In comparison with wild type control maxilla, we detected a decreased rate of cell proliferation in *Tgfbr2*$^{fl/fl}$;*Wnt1-Cre* maxilla at E14.5, but apoptosis was unaffected (Fig. 2*A*; supplemental Fig. S1, *A–D* and *F–K*). Next, we analyzed the distribution of cells throughout the cell cycle using *Tgfbr2*$^{fl/fl}$ (control) and

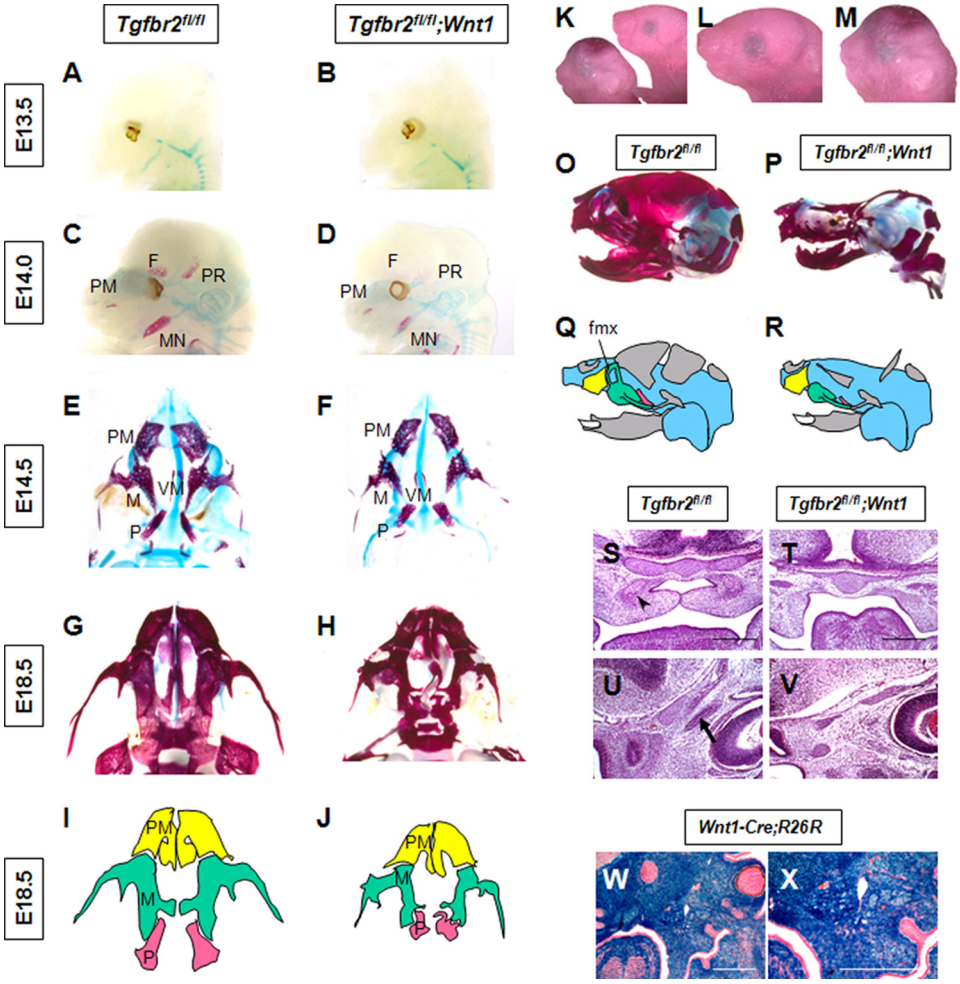

FIGURE 1. **Development of the maxilla in *Tgfbr2*$^{fl/fl}$;*Wnt1-Cre* mice.** *A–H,* whole-mount skeletal staining with Alcian blue-Alizarin Red S. Maxilla structures of *Tgfbr2*$^{fl/fl}$ (*E* and *G*) and *Tgfbr2*$^{fl/fl}$;*Wnt1-Cre* (*F* and *H*) mice are shown. The maxillary region is composed of six primordia; pairs of premaxilla, maxilla, and palatine bones, which are all derived from CNCC. The size of the maxilla and palatine bones in newborn *Tgfbr2*$^{fl/fl}$;*Wnt1-Cre* mice were smaller than those of *Tgfbr2*$^{fl/fl}$ control mice. *F,* frontal bone; *PM,* premaxilla bone; *M,* maxilla bone; *P,* palatine bone; *PR,* parietal bone; *MN,* mandible; *VM,* vomer. *I* and *J,* schematic drawings in *I* and *J* are derived from images *G* and *H,* respectively. Note that the size of the maxilla bone is decreased in *Tgfbr2*$^{fl/fl}$;*Wnt1-Cre* mice at E14.5. Premaxilla are highlighted in *yellow*, maxilla in *green*, and palatine bone in *red*. *K–M,* morphology of *Tgfbr2*$^{fl/fl}$ (*K right, L*) and *Tgfbr2*$^{fl/fl}$;*Wnt1-Cre* (*K left, M*) mice. *L* and *M* are higher magnifications of *K*. *O* and *P,* whole-mount skeletal staining with Alcian blue-Alizarin Red S of *Tgfbr2*$^{fl/fl}$ (*O*) and *Tgfbr2*$^{fl/fl}$;*Wnt1-Cre* (*P*) newborn mice. *Q* and *R,* schematic drawings in *Q* and *R* are derived from images *O* and *P,* respectively. *fmx,* frontal process of maxilla bone. *S–V,* hematoxylin and eosin staining of sections from the maxilla of *Tgfbr2*$^{fl/fl}$ (*S* and *U*) and *Tgfbr2*$^{fl/fl}$;*Wnt1-Cre* (*T* and *V*) mice. *Arrowhead* indicates the palatal process of the maxilla bone. *Arrow* indicates the frontal process of maxilla bone. *Scale bar,* 200 μm. *W* and *X,* LacZ staining of *Wnt1-Cre* mice carrying the *R26R* reporter gene. *Scale bar,* 300 μm.

Tgfbr2$^{fl/fl}$;*Wnt1-Cre* maxilla by fluorescence-activated cell sorting analyses after propidium iodide staining. We detected no significant changes in the proportion of cells at each stage of the cell cycle in *Tgfbr2*$^{fl/fl}$ and *Tgfbr2*$^{fl/fl}$;*Wnt1-Cre* maxilla from E12.5 to E14.5 (supplemental Fig. 1*E*). D-type cyclins (cyclins D1, D2, and D3) are encoded by distinct genes that are induced in a cell lineage-specific manner (26). We found that cyclin D1 expression was reduced at E13.5 and E14.5, and cyclin D3 expression was reduced at E14.5 in *Tgfbr2*$^{fl/fl}$;*Wnt1-Cre* maxilla relative to *Tgfbr2*$^{fl/fl}$ mice (Fig. 2, *B* and *C*). In contrast, there were no significant changes in the expression levels of other cyclins (Fig. 2, *B* and *C*). Gene expression of D-type cyclins is regulated by a wide array of transcriptional factors, including transactivators such as STAT proteins, NF-κB, Egr-1, Ets-2, cAMP-response element-binding protein, and c-Jun and suppressors such as peroxisome proliferator-activated receptor-γ, caveolin-1, E2F-1, Jun-B, INI1/hSNF5, and the FoxO family (26, 27). We examined the gene expression of cyclin D regulators using quantitative RT-PCR in control and *Tgfbr2*$^{fl/fl}$;*Wnt1-Cre* maxilla at E13.5 (Fig. 2, *D* and *E*). *FoxO4* and *Jun-B* were up-regulated 2-fold in *Tgfbr2*$^{fl/fl}$;*Wnt1-Cre* maxilla at E13.5, but there were no significant changes in other regulators of type D cyclins. FoxO4 protein was up-regulated at E13.5 and E14.5, a time course that correlates with the reduction of cyclin D1 protein (Fig. 2, *B*, *F,* and *G*).

To determine the activity of the JNK, we analyzed the phosphorylation of JNK by immunoblotting. JNK activity was up-regulated at E13.5 and E14.5 in *Tgfbr2*$^{fl/fl}$;*Wnt1-Cre* maxilla compared with *Tgfbr2*$^{fl/fl}$ (Fig. 2*F*). These data indicate that loss of Tgf-β signaling results in up-regulated FoxO4 expression and JNK activity, followed by decreased cyclin D expression.

Previous studies indicated that Tgf-β signaling regulates osteogenic differentiation during bone formation (28, 29). To investigate the effect of decreased proliferation activity on cell fate determination, we compared the expression of genes involved in osteogenic differentiation in *Tgfbr2*$^{fl/fl}$ (control) and *Tgfbr2*$^{fl/fl}$;*Wnt1-Cre* maxilla at E13.5 by quantitative RT-PCR. Osteopontin/*Spp1* and *Runx2* were up-regulated 3-fold in *Tgfbr2*$^{fl/fl}$;*Wnt1-Cre* maxilla at E13.5 (Fig. 3*A*). Gene expression of osteocalcin, osteonectin, and type I collagen were also up-regulated 1.5-fold in *Tgfbr2*$^{fl/fl}$;*Wnt1-Cre* maxilla at E13.5 (Fig. 3*A*). To confirm the altered osteogenic differentiation in *Tgfbr2*$^{fl/fl}$;*Wnt1-Cre* maxilla, we analyzed the expression of proteins involved in osteogenic differentiation in *Tgfbr2*$^{fl/fl}$ and *Tgfbr2*$^{fl/fl}$;*Wnt1-Cre* maxilla by immunoblotting. Expression of osteocalcin, osteopontin, and osteonectin was up-regulated in *Tgfbr2*$^{fl/fl}$;*Wnt1-Cre* maxilla at E13.5 and E14.5 (Fig. 3, *B* and *C*). Furthermore, osteogenic differentiation was up-regulated following osteogenic induction of primary MEMM cells from *Tgfbr2*$^{fl/fl}$;*Wnt1-Cre* mice compared with *Tgfbr2*$^{fl/fl}$ mice (Fig. 3*D*). Gene expression of osteopontin/*Spp1*, osteocalcin, and osteonectin was induced in *Tgfbr2*$^{fl/fl}$ MEMM cells after osteogenic induction, and these gene expres-

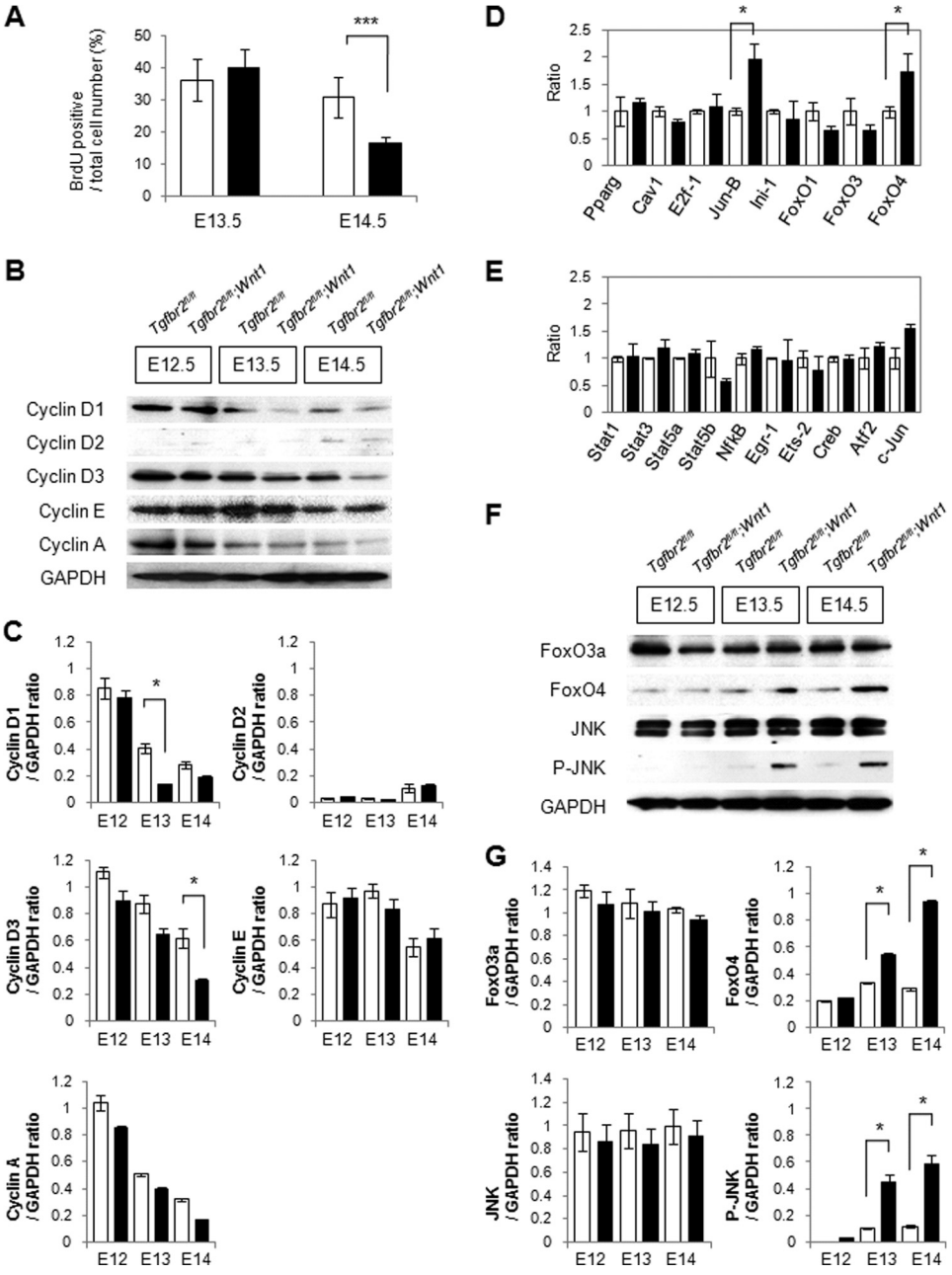

FIGURE 2. **Loss of *Tgfbr2* in CNCC results in decreased type D cyclin-dependent cell proliferation during intramembranous ossification.** *A,* ratio of bromodeoxyuridine (*BrdU*)-labeled nuclei in the maxilla of *Tgfbr2*$^{fl/fl}$ (*white bars*) and *Tgfbr2*$^{fl/fl}$;*Wnt1-Cre* (*black bars*) mice at E13.5 and E14.5. Data are mean ± S.D. values of five mice in each group. ***, $p < 0.001$. *B,* immunoblotting analysis of *Tgfbr2*$^{fl/fl}$ and *Tgfbr2*$^{fl/fl}$;*Wnt1-Cre* maxilla at E12.5, E13.5, and E14.5. Data shown are representative of three separate experiments. *C,* plot shows the ratios between cyclin D1, cyclin D2, cyclin D3, cyclin E, and cyclin A *versus* GAPDH based on quantitative densitometry of immunoblotting data in *B*; *, $p < 0.05$. *Tgfbr2*$^{fl/fl}$, *white bars*; *Tgfbr2*$^{fl/fl}$;*Wnt1-Cre*, *black bars*. *D* and *E,* quantitative RT-PCR analyses of cyclin D regulators from E13.5 maxilla of *Tgfbr2*$^{fl/fl}$ (*open columns*) and *Tgfbr2*$^{fl/fl}$;*Wnt1-Cre* (*closed columns*) mice. *, $p < 0.05$. *F,* immunoblotting analysis of FoxO family members and activated JNK in the maxilla of *Tgfbr2*$^{fl/fl}$ and *Tgfbr2*$^{fl/fl}$;*Wnt1-Cre* maxilla at E12.5, E13.5, and E14.5. Data shown are representative of three separate experiments. *G,* plot shows the ratios between FoxO3a, FoxO4, JNK, and phosphorylated JNK *versus* GAPDH after quantitative densitometry of immunoblotting data in *F*; *, $p < 0.05$. *Tgfbr2*$^{fl/fl}$, *white bars*; *Tgfbr2*$^{fl/fl}$;*Wnt1-Cre*, *black bars*.

sions were elevated in *Tgfbr2*$^{fl/fl}$;*Wnt1-Cre* MEMM cells (Fig. 3, *E* and *F*). Thus, the reduced proliferation activity in CNCC-derived osteoprogenitor cells is followed by altered osteogenic differentiation in *Tgfbr2*$^{fl/fl}$;*Wnt1-Cre* maxilla, resulting in the ossification of a reduced maxilla bone primordium at E14.5 (supplemental Fig. S4*A*).

Tgf-β Signaling Regulates Gene Expression of Basal Transcriptional Factors—Previous studies revealed that some basal transcriptional factors are expressed in a tissue- and cell-specific manner (14, 30). Mutations of these basal transcriptional factors resulted in decreased cell proliferation (15). To explore potential osteoprogenitor cell-specific regulation of basal transcriptional factors by Tgf-β signaling, we analyzed the gene expression of basal transcriptional factors in the maxilla of *Tgfbr2*$^{fl/fl}$ and *Tgfbr2*$^{fl/fl}$;*Wnt1-Cre* mice using quantitative RT-PCR. Interestingly, *Taf4b* was down-regulated in *Tgfbr2*$^{fl/fl}$;*Wnt1-Cre* maxilla at E11.5 and E12.5 (Fig. 4, *A* and *B*). Gene expression of *Taf1* was down-regulated at E12.5 but not E11.5 (Fig. 4*B*). Loss of *Taf4* results in increased gene expression of *Tgfb1*, *Tgfb3*, and *Ctgf* (9), and overexpression of *Taf4b* results in the altered gene expression of *Ctgf* and *Tgfb* ligands (9), suggesting that the transcriptional regulation of *Taf4b* and its paralogue *Taf4* is closely related to Tgf-β signaling. Taken together, these data suggest that the stoichiometry of basal transcriptional factors incorporated into TFIID regulates the fate of osteoprogenitor cells.

Taf4b Is Specifically Expressed in Maxillary Bone Primordium—*Taf4b* is specifically expressed in gonad tissues in adult mice (12, 30, 31); however, the expression pattern and function of Taf4b are still unknown during embryogenesis. To examine the expression pattern of *Taf4b* during embryonic development, we performed whole-mount *in situ* hybridization (Fig. 4, *C–H*). *Taf4b* expression was prominent in the maxilla and limbs from E10.5 to E12.5, and weaker staining was detectable in the mandible and frontal bone primordia. *Taf4b* expression was detectable in the osteogenic primordia of wild type mice at E14.5 (Fig. 4, *I–K* and *P*), but it was significantly reduced in the bone primordia of *Tgfbr2*$^{fl/fl}$;*Wnt1-Cre* mice (Fig. 4, *L–N* and *Q*). In contrast, we detected Taf1 expression throughout the craniofacial region in wild type mice and reduced expression in *Tgfbr2*$^{fl/fl}$;*Wnt1-Cre* mice at E13.5 and E14.0 (Fig. 4, *U–X*). To investigate Tgf-β

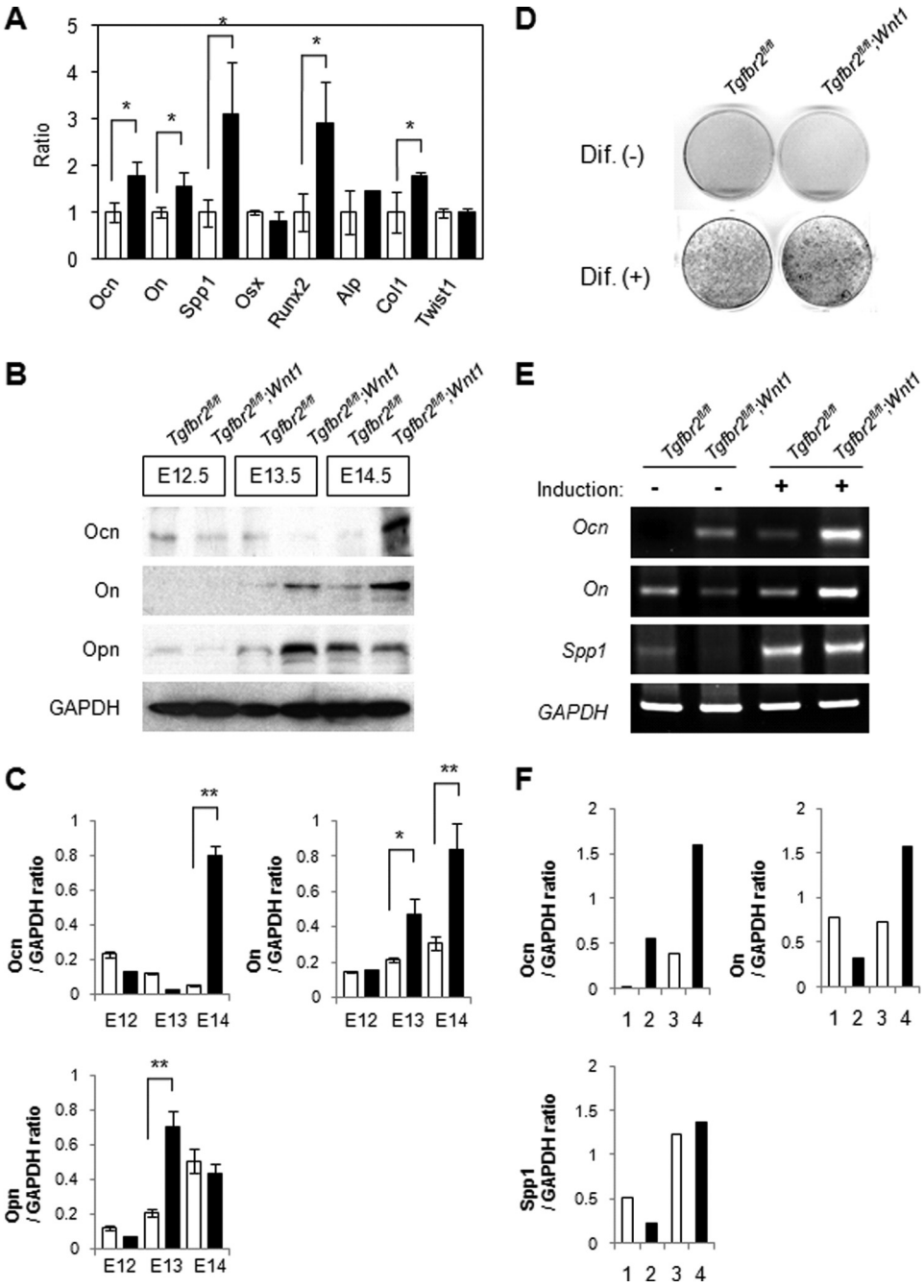

FIGURE 3. **Loss of *Tgfbr2* in CNCC results in altered osteogenic differentiation during intramembranous ossification.** *A,* quantitative RT-PCR analyses of indicated genes in *Tgfbr2*$^{fl/fl}$ (*open columns*) and *Tgfbr2*$^{fl/fl}$;*Wnt1-Cre* (*closed columns*) mice at E13.5. *Ocn*, osteocalcin; *On*, osteonectin; *Spp1*, osteopontin; *Osx*, Osterix; *Alp*, alkaline phosphatase; *Col1*, type I collagen. *, $p < 0.05$. *B,* immunological analysis of osteocalcin (*Ocn*), osteonectin (*On*), and osteopontin (*Opn*) in *Tgfbr2*$^{fl/fl}$ and *Wnt1-Cre*;*Tgfbr2*$^{fl/fl}$ maxilla at E12.5, E13.5, and E14.5. Data shown are representative of three separate experiments. *C,* plot shows the ratios between osteocalcin (*Ocn*), osteonectin (*On*), and osteopontin (*Opn*) *versus* GAPDH based on quantitative densitometry of immunoblotting data in *B*; *, $p < 0.05$. *Tgfbr2*$^{fl/fl}$, *white bars*; *Tgfbr2*$^{fl/fl}$;*Wnt1-Cre*, *black bars*. *D,* osteogenic differentiation of *Tgfbr2*$^{fl/fl}$ and *Tgfbr2*$^{fl/fl}$;*Wnt1-Cre* primary MEMM cells cultured for 14 days in osteogenic induction medium. Alkaline phosphatase (*ALP*) staining of *Tgfbr2*$^{fl/fl}$ and *Tgfbr2*$^{fl/fl}$;*Wnt1-Cre* MEMM cells cultured without (*Dif.* −) or with (*Dif.* +) osteogenic inducer for 2 weeks. *E,* mRNA expression of indicated genes after no osteogenic induction (−) or induction (+) in *Tgfbr2*$^{fl/fl}$ and *Tgfbr2*$^{fl/fl}$;*Wnt1-Cre* MEMM cells. Data shown are representative of three separate experiments. *F, graph* shows quantitative densitometry analysis of gel electrophoresis data in *E*. Data shown are representative of three separate experiments. *Lane 1, Tgfbr2*$^{fl/fl}$ MEMM cells without osteogenic induction; *lane 2, Wnt1-Cre*;*Tgfbr2*$^{fl/fl}$ MEMM cells without osteogenic induction; *lane 3, Tgfbr2*$^{fl/fl}$ MEMM cells with osteogenic induction; *lane 4, Wnt1-Cre*;*Tgfbr2*$^{fl/fl}$ MEMM cells with osteogenic induction.

regulation of *Taf4b in vivo*, we implanted beads containing Tgf-β2 protein into organ cultures of maxilla derived from *Tgfbr2*$^{fl/fl}$ and *Tgfbr2*$^{fl/fl}$;*Wnt1-Cre* mice (Fig. 4, *R–T*). At 24 h after the administration of Tgf-β2, *Taf4b* gene expression was up-regulated around the beads in controls but not in *Tgfbr2*$^{fl/fl}$;*Wnt1-Cre* maxilla (Fig. 4, *S* and *T*). Furthermore, gene expression of *Taf4b* was up-regulated following osteogenic induction of primary MEMM cells from wild type mice but not in that of *Tgfbr2*$^{fl/fl}$;*Wnt1-Cre* mice (supplemental Fig. S3). We conclude that Tgf-β signaling regulates the gene expression of *Taf4b*.

Double Knockdown of Taf4b and Taf1 Affects Gene Expression Related to Cellular Proliferation, Initiation of Bone Formation, and Osteogenic Differentiation—To test the functional significance of *Taf4b* and *Taf1* in regulating the fate of osteogenic progenitor cells, we reduced the gene expression of *Taf4b* and *Taf1* in primary MEMM cells derived from E13.5 maxilla using an siRNA knockdown approach (Fig. 5*A*). Gene expression of *Taf4b* and *Taf1* was successfully suppressed by the siRNA treatment (Fig. 5*A*). We found that the simultaneous down-regulation of *Taf4b* and *Taf1* resulted in reduced cell proliferation (Fig. 5*B*). Gene expression of *FoxO3* and *FoxO4*, which are cyclin D suppressors, was significantly increased by 1.4- and 1.5-fold after siRNA treatment of *Taf4b* alone and a 1.8- and 1.4-fold change after siRNA treatment of *Taf1* and *Taf4b* together, respectively (Fig. 5*C*). To analyze osteogenic differentiation, we cultured primary MEMM cells treated with *Taf4b*, *Taf1*, and *Taf4b/Taf1* double siRNA for 2 weeks with osteogenic induction medium and then analyzed alkaline phosphatase activity. Specifically, siRNA mixture was added every 3 days into the cell culture medium throughout the 2 weeks of culture. The success of our siRNA knockdown experiments was demonstrated by quantitative gene expres-

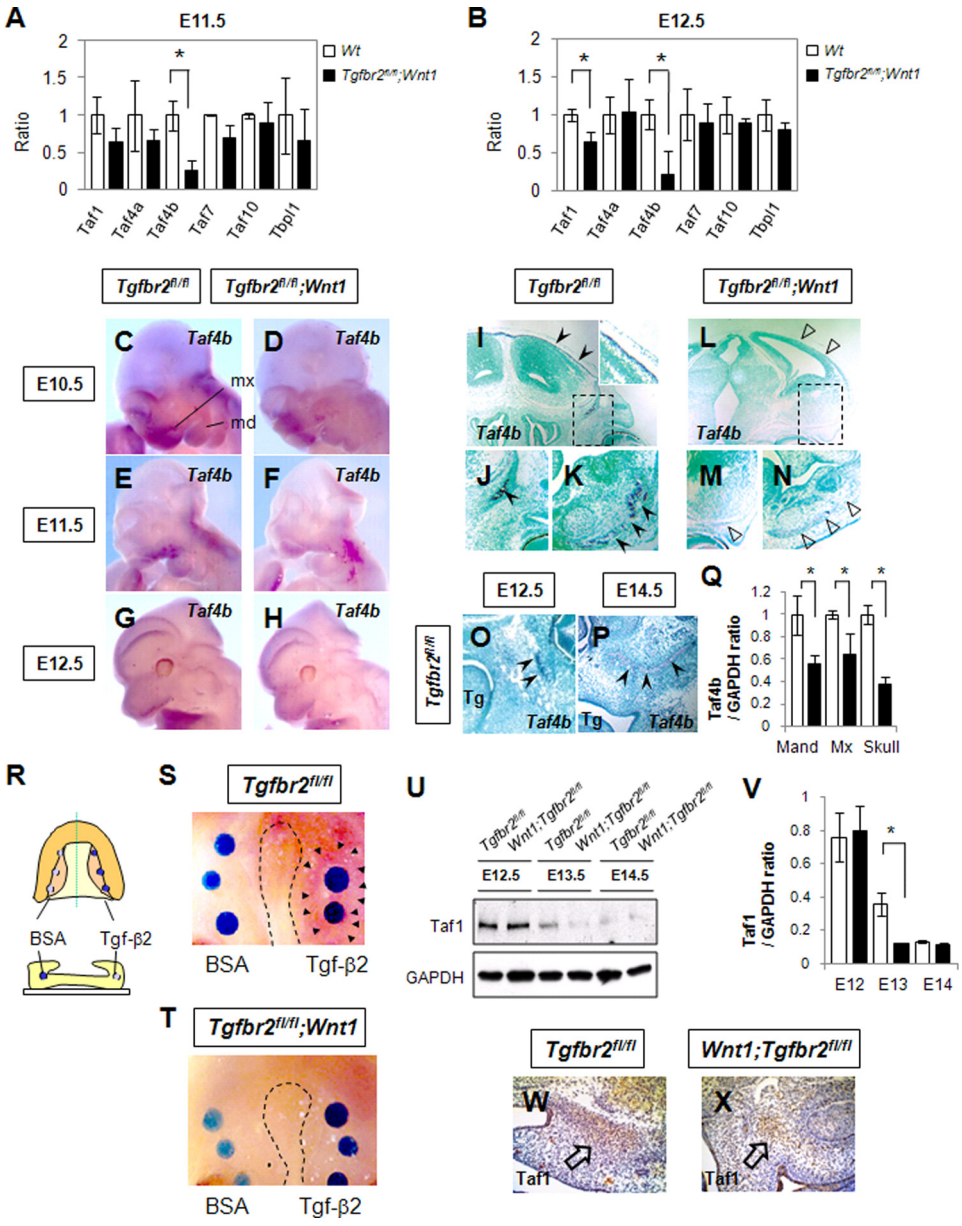

FIGURE 4. **Osteoprogenitor cell-specific expression of *Taf4b* in mouse embryos and reduced *Taf4b* expression in the maxillary process of *Tgfbr2*$^{fl/fl}$;*Wnt1-Cre* mice.** *A* and *B*, quantitative RT-PCR analyses of indicated genes in the maxilla of *Tgfbr2*$^{fl/fl}$ (*open columns*) and *Tgfbr2*$^{fl/fl}$;*Wnt1-Cre* (*closed columns*) mice at E11.5 (*A*) and E12.5 (*B*). *Wt*, wild type. *C–H*, whole-mount *in situ* hybridization of *Taf4b* in *Tgfbr2*$^{fl/fl}$ and *Tgfbr2*$^{fl/fl}$;*Wnt1-Cre* mice at E10.5, E11.5, and E12.5. *Taf4b* mRNA was strongly expressed in the maxilla and limb and weakly expressed in the mandible and frontal primordia. *mx*, maxillary process; *md*, mandibular process. *I–P*, *in situ* hybridization of *Taf4b* mRNA in sections of *Tgfbr2*$^{fl/fl}$ and *Tgfbr2*$^{fl/fl}$;*Wnt1-Cre* mice at E14.5. *Taf4b* was strongly expressed by osteoprogenitor cells in the skull, frontal bone, mandible, and maxilla of wild-type mice, whereas the gene expression of *Taf4b* was significantly reduced in *Tgfbr2*$^{fl/fl}$;*Wnt1-Cre* mice. *Boxed areas* in *I* and *L* are magnified in *J* and *M*, respectively. Wild-type maxilla of each developmental stage is shown in *O* and *P*. *Arrowheads* point to expression of *Taf4b* mRNA. *Open arrowheads* indicate areas negative for *Taf4b* expression. *Tg* is tongue. *Q*, quantitative RT-PCR analyses of *Taf4b* from E14.5 skull, mandible (*Mand*), and maxilla (*Max*) of *Tgfbr2*$^{fl/fl}$ (*open columns*) and *Tgfbr2*$^{fl/fl}$;*Wnt1-Cre* (*closed columns*) mice. *, $p < 0.05$. *R–T*, Tgf-β2 or bovine serum albumin (*BSA*) bead implantation experiment in maxillas from *Tgfbr2*$^{fl/fl}$ (*S*) and *Tgfbr2*$^{fl/fl}$;*Wnt1-Cre* (*T*) mice at E13.5. *R* is a schematic diagram of the experiment design. *Arrowheads* indicate the expression of *Taf4b* mRNA detected by whole-mount *in situ* hybridization. *Dotted line* outlines the edge of palates. *U*, immunoblotting analysis of Taf1 in *Tgfbr2*$^{fl/fl}$ and *Tgfbr2*$^{fl/fl}$;*Wnt1-Cre* maxilla at E12.5, E13.5, and E14.5. Data shown are representative of three separate experiments. *V*, plot shows the ratios between Taf1 and GAPDH after quantitative densitometry of immunoblotting data in *U*. *, $p < 0.05$. *Tgfbr2*$^{fl/fl}$ (*white bars*) and *Tgfbr2*$^{fl/fl}$;*Wnt1-Cre* (*black bars*). *W* and *X*, immunohistochemical staining of Taf1 in sections of *Tgfbr2*$^{fl/fl}$ (*W*) and *Tgfbr2*$^{fl/fl}$;*Wnt1-Cre* (*X*) mice at E14.0. Taf1 expression was significantly reduced in *Tgfbr2*$^{fl/fl}$;*Wnt1-Cre* mice. *Arrows* point to expression of Taf1.

sion analyses (Fig. 5*A*). We detected increased osteogenic differentiation in samples with combined down-regulation of *Taf4b* and *Taf4b*/*Taf1* (Fig. 5*D*). To investigate osteogenic differentiation following *Taf4b* and *Taf1* siRNA treatment, we analyzed the expression of genes related to bone formation. We found that *Spp1* was specifically up-regulated after *Taf4b* siRNA treatment but not *Taf1* siRNA treatment (Fig. 5*E*). These data confirm that *Taf4b* has unique functions in CNCC-derived osteoprogenitor cells. Interestingly, *Runx2* expression was specifically up-regulated after siRNA knock-down of *Taf4b*/*Taf1* together, although synergistic changes were not seen in other osteogenic factors, suggesting that a combination of Taf4b and Taf1 regulates the initiation of bone formation (Fig. 5*F*). Runx2 is required for mesenchymal cell differentiation into osteoblasts (32). Runx2 activates expression of several genes expressed by mature osteoblasts and chondrocytes (33, 34). Basal transcriptional factors may regulate *Runx2* gene expression via Tgf-β signaling to promote the initiation of osteogenic differentiation. Thus, basal transcriptional factors have multifunctional physiological roles in CNCC-mediated osteoprogenitor cells that include regulation of cell proliferation, osteogenic fate determination, and differentiation, and Taf1 and Taf4b work synergistically during intramembranous bone development following regulation by Tgf-β signaling (supplemental Fig. S4*B*).

DISCUSSION

We investigated CNCC-derived intramembranous bone formation and the downstream targets of the Tgf-β signaling using *Tgfbr2*$^{fl/fl}$;*Wnt1-Cre* mice. The proliferation period of osteoprogenitor cells derived from *Tgfbr2*$^{fl/fl}$;*Wnt1-Cre* mice is shorter than that of wild type mice. The consequence of the decreased proliferation term is the early onset of osteogenic differentiation. Thus, the decreased size of the maxilla in *Tgfbr2*$^{fl/fl}$;*Wnt1-Cre*

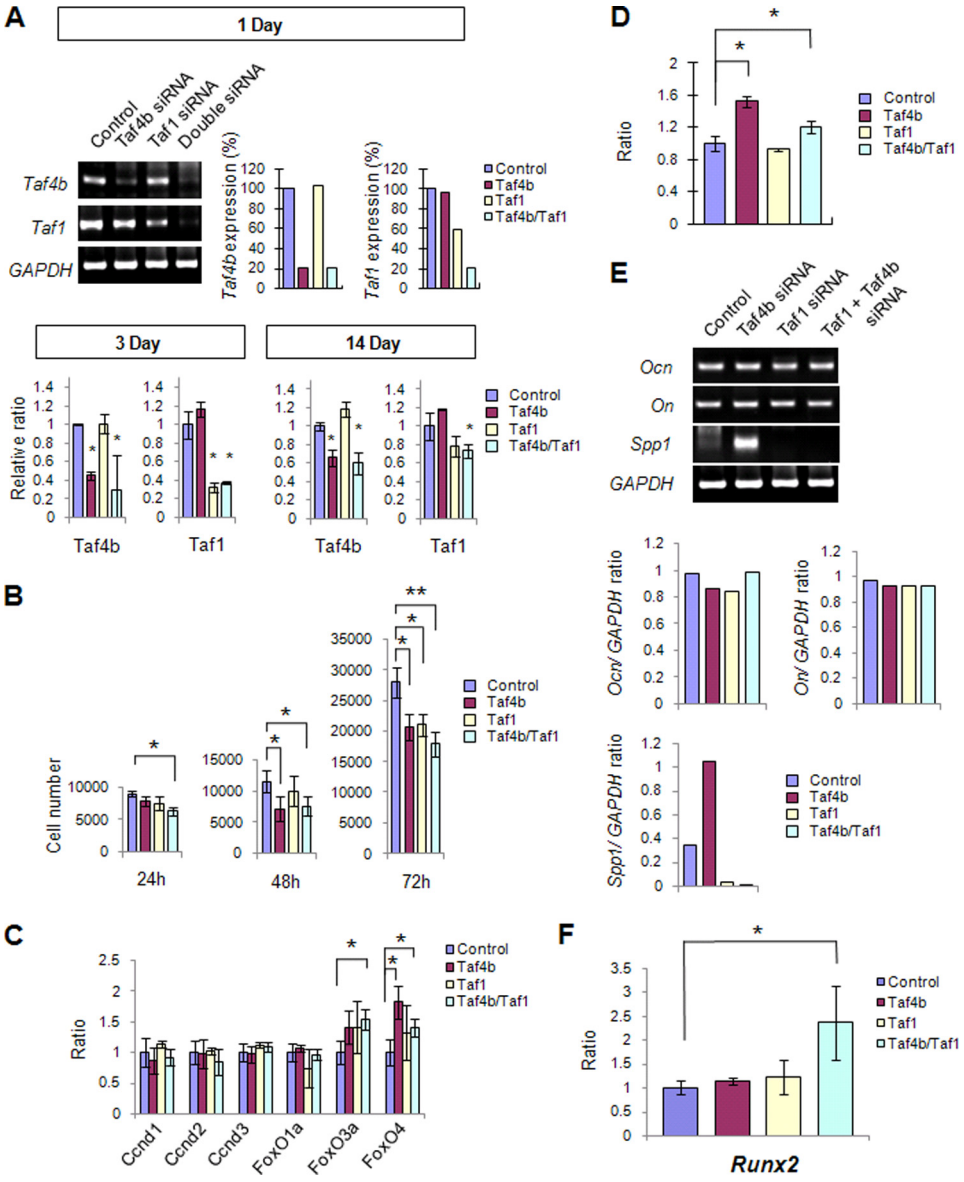

FIGURE 5. **Osteogenic progenitor cell proliferation and differentiation in primary MEMM cells after siRNA knockdown of *Taf1* and *Taf4b*.** *A, Taf4b* and *Taf1* mRNA expression in primary MEMM cells isolated from wild-type maxilla after a 24-h treatment with *Taf4b*, *Taf1*, or *Taf4b* and *Taf1* (*double*) siRNA. *, $p < 0.05$. Antisense siRNA treatment was used as control. *Graph* shows quantitative densitometry analysis of gel electrophoresis data. Data shown are representative of three separate experiments. Quantitative RT-PCR of *Taf4b* and *Taf1* was performed at 3 and 14 days during siRNA treatment. *B,* cell proliferation was assayed by cell number after siRNA treatment of MEMM cells at 24, 48, and 72 h. Cell culture was started at 5×10^3 cells (0 h). Data are the mean values from three independent experiments. *, $p < 0.05$; **, $p < 0.01$. *C,* quantitative RT-PCR of indicated genes after siRNA treatment. *, $p < 0.05$. *D,* alkaline phosphatase enzyme activities measured by β-galactosidase assay following siRNA treatments and 2 weeks culture in osteogenic induction medium. Data are expressed as ratio of absorbance at 405 nm after alkaline phosphatase staining compared with control siRNA. Alkaline phosphatase enzyme activity indicates osteogenic cell differentiation. Data are the mean values from three independent experiments. *, $p < 0.05$. *E,* mRNA expression of indicated genes after siRNA treatments. Data shown are representative of three separate experiments. *Graph* shows quantitative densitometry analysis of gel electrophoresis data. *F,* quantitation of *Runx2* mRNA level by real time RT-PCR after siRNA treatment. *, $p < 0.05$.

mice results from a decreased number of osteoprogenitor cells (supplemental Fig. S4*A*). The expression of *FoxO4* and *Runx2* was increased in *Tgfbr2*$^{fl/fl}$;*Wnt1-Cre* maxilla at E13.5 but not at E11.5 and E12.5 (supplemental Fig. S2). Moreover, after we reduced expression of *Taf4b* and *Taf1* in primary MEMM cells, we found similar changes in the expression of *FoxO4* and *Runx2,* consistent with a role for these basal transcriptional factors in regulating osteogenic gene expression. Our results suggest that Tgf-β signaling regulates the expression of basal transcriptional factors in a time- and tissue-dependent manner (supplemental Fig. S4*B*).

A previous study indicated that Taf4b mediates Tgf-β signaling more efficiently than Taf4 (9). Taf4 is ubiquitously expressed, whereas Taf4b is expressed in a tissue- and cell type-specific manner (30, 31). *Taf4* knock-out mice have premature mortality at E9.5 (9); however *Taf4b* knock-out mice show no visible phenotype except defects in gonad tissue (31). Taf4b-TFIID and Taf4-TFIID may utilize similar mechanisms to activate gene expression in the Tgf-β signaling cascade, but Taf4 can apparently compensate for the loss of Taf4b function and not vice versa. In this study, we found that *Taf1* was down-regulated in *Tgfbr2*$^{fl/fl}$;*Wnt1-Cre* maxilla at E12.5. Mutations in *Taf1* result in decreased cell proliferation *in vitro* (35, 36). Future studies of *Taf1/Taf4b* double heterozygous mutant mice may demonstrate that they recapitulate the phenotype of *Tgfbr2*$^{fl/fl}$;*Wnt1-Cre* mice. This finding underlines the importance of the stoichiometry of the Taf1/Taf4b subunits in regulating intramembranous ossification.

CNCC-derived mesenchymal cells progress through osteogenic proliferation and then commit to the transition from preosteoblastic progenitors to osteoblasts. Osteopontin and osteocalcin were up-regulated in *Tgfbr2*$^{fl/fl}$;*Wnt1-Cre* mice at E13.5. The promoter region of *Taf4b* has a putative Tgf-β-response element from −293 to −284 bp, osteocalcin motif from −521 to −513 bp, and osteopontin-response element from −149 to −135 bp, consistent with our hypothesis that gene expression of *Taf4b* is regulated by Tgf-β signaling directly and/or indirectly. Furthermore, osteogenic inducers may also provide feedback to *Taf4b* transcriptional regulation. Our study demonstrates that Tgf-β-regulated *Taf4b* gene expression is a tightly controlled process during intramembranous maxillary bone formation.

Bone formation requires a cascade of transcriptional events to control the spatial and temporal expression of osteoblast-

specific genes. Our findings show that Tgf-β signaling regulates cell proliferation and osteogenic initiation via basal transcriptional factors in osteoprogenitor cells. Tgf-β-mediated basal transcriptional factors appear to exert their functional specificity by controlling downstream target genes. Variations of the Taf(s) complex may contribute to the multifunctional role of Tgf-β signaling during embryogenesis. Thus, the interactions between Tgf-β signaling and basal transcriptional factors have a crucial function in regulating osteogenic cell proliferation and differentiation during intramembranous bone formation.

Acknowledgments—We thank H. Moses for the Tgfbr2$^{fl/fl}$ mice and Julie Mayo for critical reading of the manuscript.

REFERENCES

1. Jiang, X., Iseki, S., Maxson, R. E., Sucov, H. M., and Morriss-Kay, G. M. (2002) *Dev. Biol.* **241,** 106–116
2. Chai, Y., and Maxson, R. E., Jr. (2006) *Dev. Dyn.* **235,** 2353–2375
3. Chai, Y., Ito, Y., and Han, J. (2003) *Crit. Rev. Oral Biol. Med.* **14,** 78–88
4. Ito, Y., Yeo, J. Y., Chytil, A., Han, J., Bringas, P., Jr., Nakajima, A., Shuler, C. F., Moses, H. L., and Chai, Y. (2003) *Development* **130,** 5269–5280
5. Ross, S., and Hill, C. S. (2008) *Int. J. Biochem. Cell Biol.* **40,** 383–408
6. Müller, C., and Leutz, A. (2001) *Curr. Opin. Genet. Dev.* **11,** 167–174
7. de la Serna, I. L., Ohkawa, Y., and Imbalzano, A. N. (2006) *Nat. Rev. Genet.* **7,** 461–473
8. Hiller, M., Chen, X., Pringle, M. J., Suchorolski, M., Sancak, Y., Viswanathan, S., Bolival, B., Lin, T. Y., Marino, S., and Fuller, M. T. (2004) *Development* **131,** 5297–5308
9. Mengus, G., Fadloun, A., Kobi, D., Thibault, C., Perletti, L., Michel, I., and Davidson, I. (2005) *EMBO J.* **24,** 2753–2767
10. Metcalf, C. E., and Wassarman, D. A. (2007) *Dev. Dyn.* **236,** 2836–2843
11. Wang, X., Truckses, D. M., Takada, S., Matsumura, T., Tanese, N., and Jacobson, R. H. (2007) *Proc. Natl. Acad. Sci. U.S.A.* **104,** 7839–7844
12. Liu, W. L., Coleman, R. A., Grob, P., King, D. S., Florens, L., Washburn, M. P., Geles, K. G., Yang, J. L., Ramey, V., Nogales, E., and Tjian, R. (2008) *Mol. Cell* **29,** 81–91
13. Hampsey, M. (1998) *Microbiol. Mol. Biol. Rev.* **62,** 465–503
14. Veenstra, G. J., and Wolffe, A. P. (2001) *Trends Biochem. Sci.* **26,** 665–671
15. Davidson, I., Kobi, D., Fadloun, A., and Mengus, G. (2005) *Cell Cycle* **4,** 1486–1490
16. Albright, S. R., and Tjian, R. (2000) *Gene* **242,** 1–13
17. Lemon, B., and Tjian, R. (2000) *Genes Dev.* **14,** 2551–2569
18. Sasaki, T., Ito, Y., Bringas, P., Jr., Chou, S., Urata, M. M., Slavkin, H., and Chai, Y. (2006) *Development* **133,** 371–381
19. Iwata, J., Ezaki, J., Komatsu, M., Yokota, S., Ueno, T., Tanida, I., Chiba, T., Tanaka, K., and Kominami, E. (2006) *J. Biol. Chem.* **281,** 4035–4041
20. Kawakubo, T., Okamoto, K., Iwata, J., Shin, M., Okamoto, Y., Yasukochi, A., Nakayama, K. I., Kadowaki, T., Tsukuba, T., and Yamamoto, K. (2007) *Cancer Res.* **67,** 10869–10878
21. Komatsu, M., Waguri, S., Ueno, T., Iwata, J., Murata, S., Tanida, I., Ezaki, J., Mizushima, N., Ohsumi, Y., Uchiyama, Y., Kominami, E., Tanaka, K., and Chiba, T. (2005) *J. Cell Biol.* **169,** 425–434
22. Komatsu, M., Waguri, S., Chiba, T., Murata, S., Iwata, J., Tanida, I., Ueno, T., Koike, M., Uchiyama, Y., Kominami, E., and Tanaka, K. (2006) *Nature* **441,** 880–884
23. Sou, Y. S., Waguri, S., Iwata, J., Ueno, T., Fujimura, T., Hara, T., Sawada, N., Yamada, A., Mizushima, N., Uchiyama, Y., Kominami, E., Tanaka, K., and Komatsu, M. (2008) *Mol. Biol. Cell* **19,** 4762–4775
24. Oka, K., Oka, S., Sasaki, T., Ito, Y., Bringas, P., Jr., Nonaka, K., and Chai, Y. (2007) *Dev. Biol.* **303,** 391–404
25. Hatakeyama, Y., Tuan, R. S., and Shum, L. (2004) *J. Cell. Biochem.* **91,** 1204–1217
26. Coqueret, O. (2002) *Gene* **299,** 35–55
27. Schmidt, M., Fernandez de Mattos, S., van der Horst, A., Klompmaker, R., Kops, G. J., Lam, E. W., Burgering, B. M., and Medema, R. H. (2002) *Mol. Cell. Biol.* **22,** 7842–7852
28. Javed, A., Bae, J. S., Afzal, F., Gutierrez, S., Pratap, J., Zaidi, S. K., Lou, Y., van Wijnen, A. J., Stein, J. L., Stein, G. S., and Lian, J. B. (2008) *J. Biol. Chem.* **283,** 8412–8422
29. Seo, H. S., and Serra, R. (2009) *Dev. Biol.* **334,** 481–490
30. Dikstein, R., Zhou, S., and Tjian, R. (1996) *Cell* **87,** 137–146
31. Freiman, R. N., Albright, S. R., Zheng, S., Sha, W. C., Hammer, R. E., and Tjian, R. (2001) *Science* **293,** 2084–2087
32. Komori, T. (2002) *J. Cell. Biochem.* **87,** 1–8
33. Stricker, S., Fundele, R., Vortkamp, A., and Mundlos, S. (2002) *Dev. Biol.* **245,** 95–108
34. Yoshida, C. A., Furuichi, T., Fujita, T., Fukuyama, R., Kanatani, N., Kobayashi, S., Satake, M., Takada, K., and Komori, T. (2002) *Nat. Genet.* **32,** 633–638
35. Maile, T., Kwoczynski, S., Katzenberger, R. J., Wassarman, D. A., and Sauer, F. (2004) *Science* **304,** 1010–1014
36. Hilton, T. L., Li, Y., Dunphy, E. L., and Wang, E. H. (2005) *Mol. Cell. Biol.* **25,** 4321–4332